Frequency Analysis of Vortex Shedding in Wake Area behind the NACA0012 Airfoil via Fully-Lagrangian Vortex Elements Method

Nima Zamani Meymian[1], Behzad Ghadiri Dehkordi[2]

1. Masters Student, Aerospace Department, Faculty of Engineering, Tarbiat Modarres University, Tehran, Iran; Nima_nzm@Hotmail.com
2. Assistant Professor, Aerospace Department, Faculty of Engineering, Tarbiat Modarres University, Tehran, Iran; Ghadirib@Modares.ac.ir

Abstract

Shedding frequency of the vortices of the low-pressure area behind NACA0012 airfoil cross-section is provided for a laminar flow of an incompressible viscose fluid using Lagrangian vortex elements scheme. In the current work, only those areas of the solution domain were modeled where there are velocity gradients. It was done by the vorticity transfer equation that was obtained by calculating the cross product of the sides of the momentum equation. According to the *Fractional Step* method, the vorticity transfer equation was separated into two different equations that were solved sequentially in each time step: non-linear convection equation and the linear diffusion equation. Vorticity field in the physical domain was separated by the sheet and bubble vortices and each of the vortex elements in the solving field moved according to Biot-Savar Law and diffused according to the random walk method. The flow around the airfoil was obtained using Joukowsly mapping of the solution of the flow around a circle. This work was validated by comparing the aerodynamics force coefficients obtained from the vortex elements method with those obtained from analytical methods. Vortex shedding frequencies were calculated using the Fourier transform of the time response of the changes in the aerodynamic forces, being compared to the experimental results under the same conditions.

Keywords: Vortex Elements, Airfoil, Viscose, Incompressible, Shedding Frequency

Introduction

The vortices formed in the low-pressure area behind solid objects in incompressible viscose fluids makes the flow unstable and turbulent. Movements of these vortices downstream of the flow can apply forces with different directions, depending on the rotation directions of the vortices, to the objects in the way of the flow. The frequency of vortex shedding is important from a structural point of view where alternate forces on the structure, over time, will result in fatigue failure. Hence, it is very important to analyze the vortex shedding frequencies. In this research, the numerical simulation of the vortex generation and vortex shedding is completed using a Lagrangian scheme called Vortex Element Method (VEM). The greatest advantage of using a Lagrangian scheme is the elimination of the need for mesh, which in turn eliminates instability problems of numerical solutions, particularly for the moving boundary problems. Based on tracking a set of certain points, the Lagrangian methods explicitly investigate the movement of a fluid layer which forms the fluid flow. Unlike Eulerian methods where all the grid points have numerical values, in Lagrangian methods, it's the Lagrangian particles that determine what field cells in a free flow contain the fluid and flow information [1]. In such models, each of the movement and diffusion mechanisms is separately solved and the movement of each vortex is calculated by summing up the movement driven by these two formulations.

A very efficient Lagrangian method that has eliminated the above-mentioned drawbacks to a great extent is *Random Vortex Method*. This method is based on connecting the vorticity field to the numerical vortices, which, given the movements of the numerical vortices under two convection and diffusion mechanisms, enables the investigation of the changes in the vorticity field.

Momentum Equation

Rotation of two-dimensional fluid element is indicated in tensor form as,

$$\omega_i = -\varepsilon_{ijk}\frac{\partial u_j}{\partial x_k} = \left(\frac{\partial u_k}{\partial x_j} - \frac{\partial u_j}{\partial x_k}\right) \tag{1}$$

Considering the potential function and flow function definitions for the basic flows, the following relations are defined to obtain φ and ψ of a vortex.

$$u = \frac{\partial \psi}{\partial y} \qquad v = -\frac{\partial \psi}{\partial x} \tag{2}$$

By replacing (2) with velocity values in (1), Poison's second-order equation is obtained as,

$$\Delta\psi = -\omega \tag{3}$$

Equation (3) is a non-homogeneous partial differential equation the solution of which can be obtained using the Green functions.

$$\psi(x) = \int G(x - \acute{x})\omega(\acute{x})dA \tag{4}$$

where $r^2 = x^2 + y^2$, $dA = dxdy$, and $X = (x, y)$.

Also,

$$G(x) = \frac{-1}{2\pi} Ln\, r \tag{5}$$

By combining relations (4) and (5) and replacing the result in (2), the velocity distribution in each point of the vorticity field is calculated, which is known as Biot-Savart Law.

$$u(x) = \int K\left(X - \acute{X}\right)\omega(\acute{X})d\acute{X} \tag{6}$$

$$K(X) = \frac{-1}{2\pi}\frac{(y,-x)}{r^2} \tag{7}$$

In which *K* is the distribution function. The vorticity field caused by the velocity gradients can be discretized using individual vortices. The vorticity applied by each vortex is viewed as a function of the core radius δ [2].

$$(X) = \sum_{i=1}^{n} \Gamma_i f_\delta(X - X_i) \tag{8}$$

where f_δ is the rotation distribution function in the core and Γ_i is the strength of vortex *i*. By replacing (5) in (4), the induced velocity of each point due to all vortices diffused in the solution domain is calculated as,

$$u_\delta(X) = \sum_{i=1}^{n} \Gamma_i K_\delta(X - X_i) \tag{9}$$

$$K_\delta(X) = \frac{1}{2\pi}\frac{(y,-x)}{r^2} k\left(\frac{r}{\delta}\right) \tag{10}$$

$$k(r) = 2\pi \int r f(r) dr \tag{11}$$

Using the velocity distribution in the Rankin vortex model, the velocity induced in each point of the solution domain due to individual vortex *i* is obtained as,

$$u_i = -\frac{1}{2\pi}\sum_{j=1}^{n} \Gamma_j \frac{y_i - y_j}{r_{ij}^2} - \frac{1}{2\pi}\sum_{j=1}^{n} \Gamma_j \frac{y_i - y_j}{r_{ij}.\delta} \tag{12}$$

$$v_i = \frac{1}{2\pi}\sum_{j=1}^{n} \Gamma_j \frac{x_i - x_j}{r_{ij}^2} + \frac{1}{2\pi}\sum_{j=1}^{n} \Gamma_j \frac{x_i - x_j}{r_{ij}.\delta} \tag{13}$$

where *n* is the number of vortex and $r_{ij} = \sqrt{\left(x_i - x_j\right)^2 + \left(y_i - y_j\right)^2}$ is the distance between two vortex centers. As it is seen in (12) and (13), if $r_{ij} \geq \delta$, we use the first part of the equations, otherwise, we will use the second part of the equations. Knowing the velocity of each vortex, its movement can be calculated with the movement mechanism of each time step.

Diffusion

The diffusion equation is solved by the random walk method. This method is based on the principle that all the vortex elements in the solution domain are exposed to the movements with a random value, such that the vortex diffusion caused by this movement satisfies the vorticity diffusion equation in the continuous fluid field, which is introduced by the following relation in the cylindrical coordinate:

$$\frac{\partial \omega}{\partial t} = \upsilon \left\{ \frac{\partial^2 \omega}{\partial r^2} + \frac{1}{r} \frac{\partial \omega}{\partial r} \right\} \tag{14}$$

The analytical solution of the above equation is the relation of vorticity distribution in time and location introduced by Batchelor as [14]:

$$\omega(r,t) = \frac{\Gamma}{4\pi \nu t} e^{(-r^2/4\nu t)} \tag{15}$$

Equation (15) gives the radial distribution of vorticity at time *t*. For the vortices with the strength of unit divided into *N* smaller vortices, we assume that *n* of *N* elements are located in a region with the area of $r.\Delta\theta.\Delta r$ at time *t*. Thus, the total vorticity, P, in this region of the field will be,

$$p = \frac{n}{N} = \left[\frac{1}{4\pi \nu t} e^{(-r^2/4\nu t)} \right] r \, \Delta\theta \, \Delta r \tag{16}$$

In other words, it can be said that P is the possibility of a vortex element being in a region of the field with the area of r.Δθ.Δr after distribution. Therefore, element i has to be moved by r_i and θ_i in the radial and angular directions, respectively, by time t, such that the radial distribution possibility introduced by (16) is satisfied for all the r.Δθ.Δr regions that form the total of the flow field. It is obvious that the vortices are diffused with the same possibility in all the angles due to the symmetric radial movement. Thus, θ_i is defined independently of r_i as

$$\theta_i = 2\pi Q_i \tag{17}$$

where Q_i is a random number from 0 to 1. To calculate radial vortex diffusion, equation (16) is integrated from 0 to 2π. The following equation is obtained:

$$\acute{p} = \left\{ \frac{1}{2\nu t} e^{(-r^2/4\nu t)} \right\} r \, \Delta r \tag{18}$$

where $\acute{p}$ is the possibility of a vortex element present in a ring or inner and outer radiuses r and r+Δr, respectively. A better application of it is in the investigation of the possibility of a vortex in a circle with the radius of r, for which (18) is integrated from 0 to r for vortex i.

$$P_i = 1 - e^{(-r_i{}^2/4\nu t)} \tag{19}$$

P should be a number from 0 to 1 with the same possibility for all the numbers. For this purpose, a random number is produced for P from 0 to 1. Using (19), the following relation is derived from the radial vortex diffusion [5].

$$r_i = \{4\nu t \, ln(1/P_i)\}^{\frac{1}{2}} \tag{20}$$

Ultimately, the diffusion of N elements forming a vortex with the strength of one is calculated by selecting N random numbers from 0 to 1 for P_i and Q_i to be used in (17) and (19).

The vortex movement driven by the diffusion mechanism is summed up with the movement caused by the movement mechanism to obtain the total movement of the vortices in each time step as,

$$x(t+\Delta t) = x(t) + \sum_{j=1}^{n} u_i dt + \eta_x \tag{21}$$

$$y(t+\Delta t) = y(t) + \sum_{j=1}^{n} v_i dt + \eta_y \tag{22}$$

where η_x and η_y are diffusion mechanism-driven movements. It should be noted that η_x and η_y are cause by both factors. The former is the velocity induced by other individual vortices in the solution field, which is calculated by Biot-Savart law, while the latter is the velocity caused by the potential flow.

Boundary Conditions

The boundary conditions in this problem are the angular and radial velocities being 0 on the object surface. Conformal mapping technics are employed to transform the flow around the airfoil into flow around a cylinder to satisfy the boundary conditions and calculate the velocities of the points for the flow around the airfoil. This is done to satisfy the boundary condition of radial velocity equal to zero. The vortex reflection method can be applied for the flow around the cylinder [6]. In this method, if there is a vortex in the distance r from a circle with the radius of r, to satisfy the mentioned boundary condition, two mirror vortices are considered, one at $\frac{a^2}{r}$ distance from the circle center with the same strength and opposite quantity (negative/positive) of the initial vortex, and the other at the circle center with the same quantity as the initial vortex. Taking into account the effect of the addition of this vortex to the vortex set, the velocity of each individual vortex in the domain changes as

$$u_i = u_p + u_\omega + u_{\omega i1} + u_{\omega i2} \tag{23}$$

$$v_i = v_p + v_\omega + v_{\omega i1} + v_{\omega i2} \tag{24}$$

Index ω_{i1} represents the induced velocity of the mapped vortex at distance of $\frac{a^2}{r}$, and the index ω_{i2} denotes the induced velocity of the vortex at the circle center. These indexes are calculated by (12) and (13). The potential velocities are calculated as

$$u_p = \left[1 - \frac{a^2(x_i^2 - y_i^2)}{(r_i^2)^2}\right] u_\infty \tag{25}$$

$$v_p = -\left[\frac{2x_i y_i a^2}{(r_i^2)^2}\right] u_\infty \tag{26}$$

Planar vortices are employed to satisfy the no-slip condition. This condition can be satisfied by vorticity creation on the boundary. u_0 is the angular velocity component on the object boundary, which is induced by the vortices. If $u_0 \neq 0$, we create planar vortices with the power of u_0 on the boundary. These vortices are separated from the boundary and moved to the downstream by the diffusion mechanism. Until the radial distance Δs from the cylinder, the vortices are considered as sheet vortices. They are considered to be bubble ones out of this distance. In other words, each bubble vortex is produced by a sheet vortex with a length of h. Thus, the strength of the bubble vortices are $\Gamma_i = u_0 \,.\, h$, and those in sheet form are $\xi_j = \frac{\Gamma_j}{h}$ [3].

Force Coefficients

Lift and drag forces applied to an airfoil are produced by two causes: the fluid viscosity and the pressure of the fluid passing on the airfoil. Fig. 1 represents these forces and their directions.

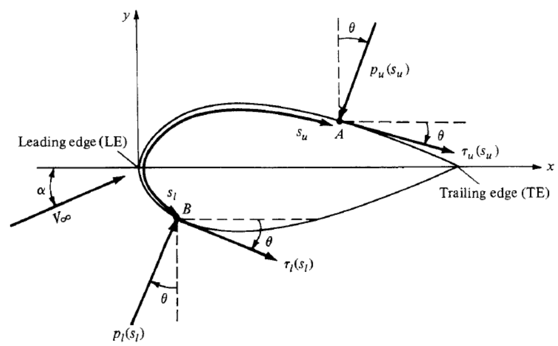

Fig. 1 Forced Applied to Airfoil and Their Directions

The viscosity-driven forces can be balanced in vertical and horizontal directs considering the shear stress direction the fluid applied to the object.

$$C_{Dv} = \frac{\tau A \sin\theta}{\frac{1}{2}\rho u_\infty^2} \tag{27}$$

$$C_{Lv} = \frac{\tau A \cos\theta}{\frac{1}{2}\rho u_\infty^2} \tag{28}$$

Using the viscosity-shear stress relation of the Newtonian fluids and combining it with (1), viscosity force coefficients are calculated for element *i* as

$$C_{Dv_i} = \frac{\mu \omega_i \Delta S_i \sin\theta_i}{\frac{1}{2}\rho u_\infty^2} \tag{29}$$

$$C_{Lv_i} = \frac{\mu \omega_i \Delta S_i \cos\theta_i}{\frac{1}{2}\rho u_\infty^2} \tag{30}$$

General lift and drag coefficients of the airfoil are obtained by algebraically summing up these coefficients for all the elements. According to the Fractional Step Method, after solving the convection and diffusion equations in a time step, the Navier-Stokes equation reduces to the following form:

$$\frac{\partial u}{\partial t} = -\frac{1}{\rho}\frac{\partial p}{\partial s} \tag{31}$$

where *u* is the angular fluid velocity on the object's surface. According to the previous statements, the angular velocity for each point on the surface will be the power of the vortex sheet. Thus, the pressure gradient on the surface based on the vortex sheet strength will be,

$$\frac{\partial p}{\partial s} = -\rho\frac{\partial \gamma}{\partial t} \tag{32}$$

In which case, the pressure change for panel *i* is written as

$$\Delta P_i = -\rho\frac{\Delta \Gamma_i}{\Delta t} \tag{33}$$

where $\Delta\Gamma_i = \Delta\gamma_i \Delta s_i$. To calculate the pressure for any point on the surface, relation (33) can be directly integrated as

$$P_m = P_1 + \sum_{n=1}^{m} \Delta P_n = P_1 - \frac{\rho}{\Delta t}\sum_{n=1}^{m} \Delta\Gamma_n \tag{34}$$

Relation (34) expresses the relative pressure of point m on the basis of a reference point with the pressure of P_1. This point is the stagnation point of the leading edge of the airfoil, which can be calculated by Bernoulli relation and upstream flow properties.

Results

Fig. 2 indicates small vortices diffusion for the downstream low-pressure region and the formation of large vortices along with their formation time intervals at the leading angle of 15° [8]. It can be seen in this figure that the concentration of the vortices formed on the airfoil surface (shear layer thickness) on top of the airfoil is greater than at the bottom of it. This shows the presence of velocity gradients and rotating flows on top of the airfoil. Due to the difference between the high and low pressures of the airfoil, and consequently, the difference in the induced velocity between the top and bottom of the airfoil, the vortices formed on the two surface parts are different. This causes the dominant flow to form larger vortices in the place where the two vortex streams meet as they move. While rotating, these vortices move toward the downstream. The street of the large vortices can be seen in Fig. 2.

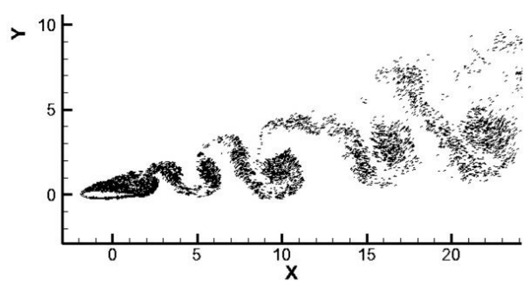

Fig. 2 Vortex Diffusion at 1m/s, *t*=80s, and Reynolds number 5000

Each point represents a singular vortex. The flow lines are drawn in Fig. 3 indicate the formation, growth, strength enhancement, and separation of the vortices. It also shows the vortices are shed into wake area downstream of the flow. Smaller vortices are attracted and absorbed by their adjacent large vortices if their rotation directions are the same.

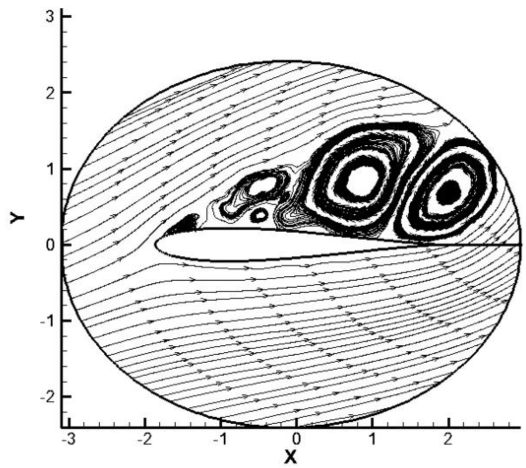

Fig. 3 Vortex Formation at Reynolds of 5000 and Leading Angle of 15°

To validate the current work, we compared the aerodynamic forces applied to the airfoil with the results obtained from an analytical solution embedded in an academic *Xfoil software* [9]. This software analytically performs airfoil calculations for viscose flow on the basis of the boundary layer equations and flow regime instabilities using Orr-Sommerfeld equations. Figs. 4, 5, and 6 demonstrate the diagrams of the variations in the lift, drag, and torsional moment coefficients versus leading angle at Reynolds 1000. The high convergence accuracy of the vortex elements method is seen in Figs. 4, 5, and 6.

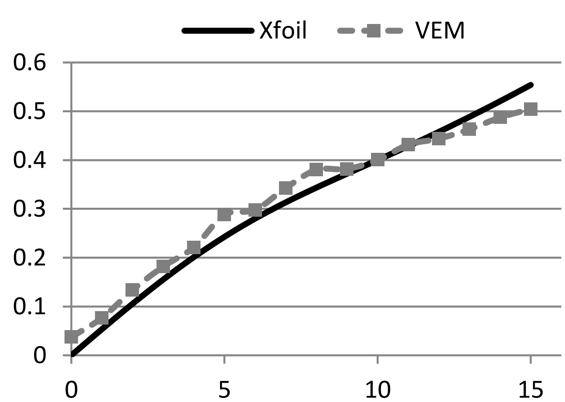

Fig. 4 Variations in Lift Force (Vertical Axis) versus Leading Angle (Horizontal Axis) at Reynolds 1000

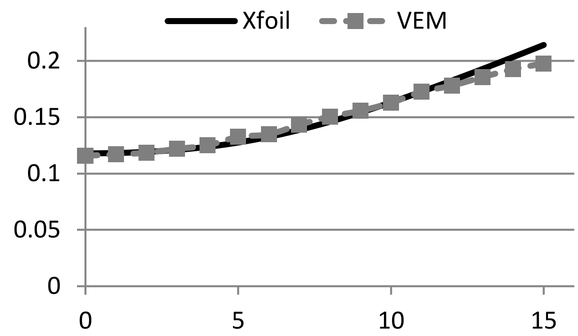

Fig. 5 Variations in Drag Force (Vertical Axis) versus Leading Angle (Horizontal Axis) at Reynolds 1000

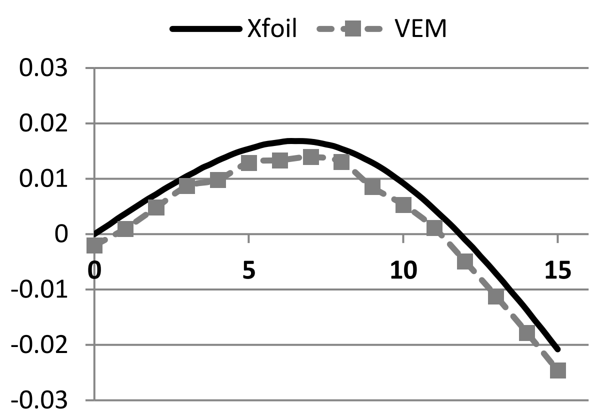

Fig. 6 Variations in Torsional Moment (Vertical Axis) versus Leading Angle (Horizontal Axis) at Reynolds 1000

Comparison of the lift and drag coefficients of the VEM with Xfoil results shows the high accuracy of the random vortex method in the investigation of vortex flow dynamics. The lift coefficient increases as the leading angle increases, which can be viewed to be because of the increased compressive force effects on the airfoil. Moreover, the difference in the pressure of the top and bottom of the airfoil increases as the leading angle increases. This, in turn, increases the lift force. The increase in the drag force induced by the increased leading angle can also be viewed as a result of the dominance of the compressive force effects. The torsional moment around the airfoil first increases due to an increase in the drag force effects on the torsional moment production. As the velocity gradients on the top airfoil surface enhance, the flow separates from the airfoil, which, in turn, leads to the reduced torsional moment.

Fourier transformation was used to analyze the vortex shedding frequencies of downstream flow. For this purpose, the variations in the lift or drag coefficients in the time domain are transferred to the frequency domain using MATLAB. Fig. 7 represents the dominant vortex shedding frequency for the leading angle 5° at Reynolds 500. As it is seen, it is 0.0392Hz. This can be done for all the states to calculate the dominant frequency. Having the frequencies, the related Strouhal number can be calculated. Fig. 8 shows the variations in Strouhal number versus Reynolds number at the leading angle 5°. The results are compared to the experimental ones in this figure. Strouhal number variation has a positive slope, which is in a good agreement with the experimental results. As previously mentioned, the change in Strouhal number, or in another word, the change in vortex shedding frequency is because of the higher flow instability at higher Reynolds numbers, the increased difference in the fluid layer velocities, and the rapider vortex formation, which, in turn, reduces the time interval between the formation and shedding of the vortices in the flow trail.

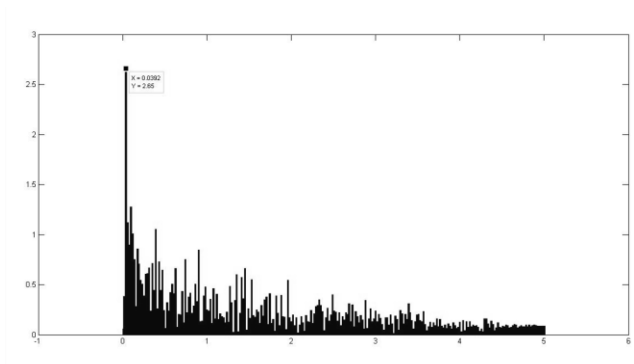

Fig. 7 Dominant Shedding Frequency of the Vortices Formed on the Airfoil Surface at Leading Angle 5° and Reynolds 500

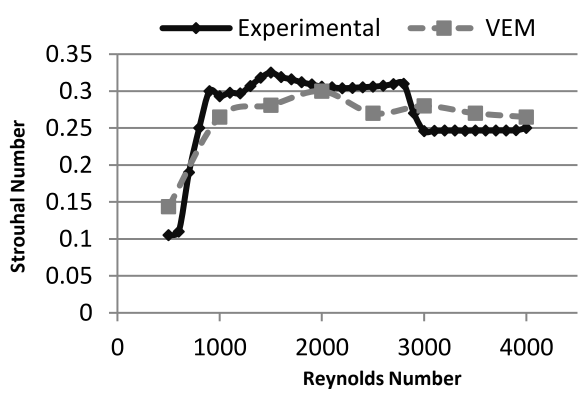

Fig. 8 Strouhal Number versus Reynolds Number

Conclusion

Vortex Elements Method (VEM) was employed in this work to model the incompressible viscose flow around a fixed NACA0012 Airfoil. To obtain the physics of the flow around the airfoil, the conformal mapping of the flow around a cylinder was used using Joukowsky mapping. Use of conformal mapping limits the geometry of the problem to some extent but simplifies the application of the boundary conditions. Comparison of the results of the current study obtained for the stationary airfoil with Xfoil results showed a high consistency between the VEM and the real-life results. Due to the inverse relationship between the diffusion mechanism calculations accuracy and the Reynolds number, the accuracy reduced as the Reynolds number increased.

For the flows at low velocities (approximately 1m/s), the vortex shedding frequency is almost unchanged, being 0.04Hz. Strouhal number of this frequency is approximately 0.25. For low leading angles, a change in the leading angle by below 10° leads to an increase in Strouhal number. Furthermore, the vortex shedding frequency enhancement gradient increases as the free flow velocity increases.

Resources

[1]- *Mark J. Stock: "Summary of Vortex Method Literature", 2007*

[2] *Chorin A. J., Bernard P. S., "Discretization of Vortex Sheet With an Example of Roll-Up", Journal of Computational Physics, 13, 1980, PP 423-429*

[3]- *Chorin A.J, "Numerical study of slightly viscous flow", Journal of fluid mechanics, Vol 57, 1973, PP 785-796.*

[4] *Batchelor G. K., "An Introduction to Fluid Dynamics", Cambridge University Press, 1970*

[5]- *Lewis, I.R., "Vortex element method for fluid dynamic analysis of engineering systems", Cambridge university press, 2003*

[6] *Katz, Poltkin, "Low-Speed Aerodynamics", McGraw Hill, 1991*

[7]- *Currie I. G., "Fundamental Mechanics of Fluids", Marcel Dekker Inc., Third Edition, 2003*

[8] Zamani Meymian, N. & Ghadiri, B. "Numerical Solution of the Viscose Flow around the Vibrating Airfoil by Vortex Elements Method", Master Thesis, Tarbiat Modarres University, Tehran, Iran, 2012

[9]- *Http://web.mit.edu/drela/Public/web/xfoil/*

[10]- *Han-Wen Lee, "Frequency Selection of Wake Flow For Naca 0012", J. Marine Science, Vol. 6, 1998*